Numerical Simulation of Cloud–Clear Air Interfacial Mixing: Homogeneous versus Inhomogeneous Mixing

MIROSLAW ANDREJCZUK*

Los Alamos National Laboratory, Los Alamos, New Mexico

WOJCIECH W. GRABOWSKI

National Center for Atmospheric Research,+ Boulder, Colorado

SZYMON P. MALINOWSKI

University of Warsaw, Institute of Geophysics, Warsaw, Poland

PIOTR K. SMOLARKIEWICZ

National Center for Atmospheric Research,+ Boulder, Colorado

(Manuscript received 19 September 2008, in final form 7 January 2009)

ABSTRACT

This note presents an analysis of several dozens of direct numerical simulations of the cloud–clear air mixing in a setup of decaying moist turbulence with bin microphysics. The goal is to assess the instantaneous relationship between the homogeneity of mixing and the ratio of the time scales of droplet evaporation and turbulent homogenization. Such a relationship is important for developing improved microphysical parameterizations for large-eddy simulation of clouds. The analysis suggests a robust relationship for the range of time scale ratios between 0.5 and 10. Outside this range, the scatter of numerical data is significant, with smaller and larger time scale ratios corresponding to mixing scenarios that approach the extremely inhomogeneous and homogeneous limits, respectively. This is consistent with the heuristic argument relating the homogeneity of mixing to the time scale ratio.

1. Introduction

The impact of entrainment and cloud–clear air mixing on the spectra of cloud droplets remains an important yet still unresolved issue in cloud physics. Because warm (ice-free) clouds are close to water saturation, conservation of the total water and moist static energy is sufficient to determine the temperature, water vapor, and cloud water mixing ratios of the homogenized mixture of cloudy and cloud-free unsaturated air. Predicting the evolution of a cloud droplet spectrum, on the other hand, requires additional constraints because, as far as bulk conservation principles are concerned, cloud water after homogenization can be distributed over either a large number of small droplets or a small number of large droplets. The concentration and size of cloud droplets critically depend on whether the mixing is homogeneous (i.e., all droplets are exposed to the same subsaturation during mixing) or inhomogeneous (i.e., the degree of droplet evaporation varies; Baker and Latham 1979; Baker et al. 1980; Burnet and Brenguier 2007). In the homogeneous mixing scenario, the number of droplets does not change and the mean droplet size decreases. In the extreme inhomogeneous mixing scenario, droplets from a fraction of the cloudy volume evaporate completely to bring the mixture to saturation, and the droplets from the rest of the cloudy volume are dispersed over the combined volumes without changing their size. It follows that the extremely inhomogeneous mixing is associated with the change of

* Current affiliation: School of Earth and Environment, University of Leeds, Leeds, United Kingdom.

+ The National Center for Atmospheric Research is sponsored by the National Science Foundation.

Corresponding author address: Wojciech W. Grabowski, NCAR/MMM, P.O. Box 3000, Boulder, CO 80307–3000.
E-mail: grabow@ncar.ucar.edu

DOI: 10.1175/2009JAS2956.1

droplet concentration, but not the droplet size. The homogeneous mixing and the extremely inhomogeneous mixing set the limits for all possible mixing scenarios. Whether cloud dilution is associated with homogeneous or inhomogeneous mixing has been shown to significantly affect radiative properties of stratocumulus (Chosson et al. 2007) and shallow convective clouds (Grabowski 2006; Slawinska et al. 2008).

The mixing scenario (i.e., the homogeneity of mixing) depends on the relative magnitude of the two time scales: the time scale of droplet evaporation and the time scale of turbulent homogenization (see discussion and references in Burnet and Brenguier 2007). If the droplet evaporation time scale is much larger than the time scale of turbulent homogenization, the mixing is expected to be close to homogeneous. In the opposite limit (i.e., when the droplet evaporation time scale is much smaller than the time scale of turbulent homogenization), the mixing is supposed to be close to the extremely inhomogeneous.

Evaporation of cloud droplets occurs near the cloud–clear air interface, where the molecular diffusion (of water vapor and temperature) and sedimentation of cloud droplets determine mean conditions for droplet evaporation. It follows that the droplet evaporation time scale $\tau_{\rm evap}$ should depend on both the droplet radius r and the relative humidity (RH) of clear air (Burnet and Brenguier 2007 and references therein):

$$\tau_{\rm evap} \equiv r\left(\frac{dr}{dt}\right)^{-1} = \frac{r^2}{A(1-{\rm RH})}, \qquad (1)$$

where $A \approx 10^{-10}$ m^2 s^{-1} is the constant in the droplet diffusional growth equation $dr/dt = AS/r$, and $S = {\rm RH} - 1$ is the supersaturation.[1] Equation (1) implies that $\tau_{\rm evap} \approx 1$ s for RH = 0.1 and $\tau_{\rm evap} \approx 10$ s for RH = 0.9 for a droplet with the radius $r = 10$ μm. The time scale of turbulent homogenization $\tau_{\rm mix}$ can be approximated by the eddy turnover time of an eddy with spatial scale equal to the size L of the volume under consideration (Baker and Latham 1979; Burnet and Brenguier 2007 and references therein):

$$\tau_{\rm mix} \equiv \frac{L}{U(L)} \sim \left(\frac{L^2}{\epsilon}\right)^{1/3}, \qquad (2)$$

where $U(L) \sim (\epsilon L)^{1/3}$ is the eddy velocity scale estimated from the turbulent kinetic energy (TKE) dissipation rate ϵ. Assuming a typical value $\epsilon = 0.01$ m^2 s^{-3} (e.g., Siebert et al. 2006), the turbulent homogenization time scale is $\tau_{\rm mix} \approx 0.2$ s for $L = 1$ cm, 5 s for $L = 1$ m, and 100 s for $L = 100$ m. Based on the scaling arguments, mixing should be therefore extremely inhomogeneous at scales resolved by large-eddy simulation (LES) models with model grid length of tens of meters, whereas it should approach the homogeneous limit at scales resolved in direct numerical simulation (DNS).

In the heuristic model of turbulent mixing proposed by Broadwell and Breidenthal (1982), the spatial scale of cloudy and clear air filaments gradually decreases, from the scale characterizing the initial engulfment of the ambient fluid, through the filamentation of cloudy and clear-air volumes (i.e., the process of turbulent stirring), down to scales characterizing the small-scale homogenization (i.e., the Batchelor and Kolmogorov scales) (e.g., Grabowski 2007; Malinowski et al. 2008). In such a case, the length scale L in (2) can be taken as a filament scale, and the mixing characteristics in an LES model should evolve from the extremely inhomogeneous at the initial stages of the mixing with large L, toward the homogeneous mixing close to microscale homogenization with L approaching the Batchelor scale. During the turbulent stirring phase, the mean size of cloud droplets remains approximately constant and the *mean* concentration (over the engulfment scale) becomes reduced because of the presence of cloudy and clear air filaments. Within cloudy filaments, however, the *local* droplet concentration remains close to the concentration of the initial cloudy air. Such a scenario is consistent with cloud observations—for instance, section 5 of Paluch and Baumgardner (1989), Figs. 1 and 2 and the accompanying discussion in Malinowski and Zawadzki (1993), and Malinowski et al. (1994)—and appears to be responsible for the observed mixing characteristics in natural clouds, often close to the extremely inhomogeneous (e.g., Blyth and Latham 1991; Haman et al. 2007; Gerber et al. 2008).

The DNS results of cloud–clear interfacial mixing with detailed microphysics (Andrejczuk et al. 2004, 2006, hereafter A04 and A06, respectively) are consistent with the Broadwell and Breidenthal model. In these simulations, the initial cloudy and clear air filaments as well as velocity perturbations are specified at scales comparable to the size of the computational domain ($\sim$1 m^3). The ensuing turbulent mixing leads to the development of smaller scales as represented by the decrease of the Taylor microscale (see Fig. 9 in A04), the decrease of the mean scale of cloudy filaments (Fig. 1, to be discussed later), and eventual microscale homogenization. These processes are also characterized by the initial increase and subsequent decrease (dissipation)

[1] If the cloudy volume were uniform to begin with, than the appropriate time scale would be the phase relaxation time scale that depends on the mean droplet radius and droplet concentration (Squires 1952; Clark and Hall 1979). For the cloud–environment mixing, however, the scale given by (1) is more relevant.

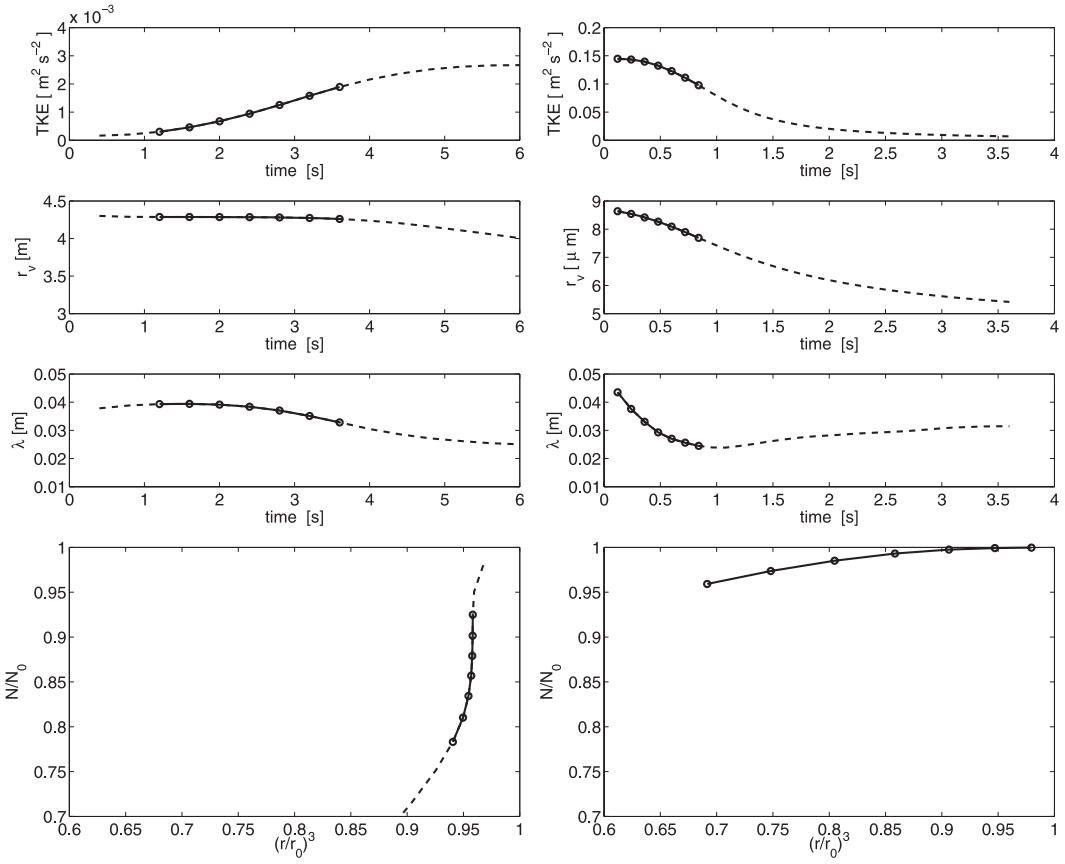

FIG. 1. (top) Evolution of the mean TKE, mean volume radius, and mean scale of cloudy filaments λ in simulations (left) B7 with RH = 30% and (right) B3 with RH = 30%. (bottom) Corresponding *r–N* diagrams. In each panel, the dots mark time levels with data used in the analysis; the dashed lines show evolutions not considered in the analysis.

of the enstrophy, in agreement with dry simulations of Herring and Kerr (1993) that motivated the modeling setup in A04 and A06. The key point of this note is to show that the homogeneity of mixing can be diagnosed from DNS at any instant during this chain of events.

As discussed in A04 and A06, the homogeneity of mixing is represented by the slope of the line depicting the evolution of the total number of droplets plotted against the mean volume radius cubed, both normalized by the initial values (see the bottom panels of Fig. 1). Such a diagram, referred to as the *r–N* diagram in A04 and A06, was used to represent the evolution of mean microphysical properties as simulated by the numerical model. In this diagram, the homogeneous mixing corresponds to the horizontal line (i.e., changing droplet size without changing the number of droplets; the zero slope), whereas the vertical line (reduction of the number of droplets without changing the size; the slope approaching infinity) implies extremely inhomogeneous mixing. The main goal of the current study is to obtain a relationship between the instantaneous ratio of the two time scales and the instantaneous slope of the line representing microphysical evolution on the *r–N* diagram, with all relevant parameters (e.g., droplet size, RH of the cloud-free air, TKE, etc.) representing volume-averaged quantities from the DNS simulation. Such a relationship can be useful for subgrid-scale parameterizations of high-spatial-resolution LES models as discussed in section 4.

The time scale ratio discussed above, known as the Damkoehler number in the turbulent combustion and chemical engineering communities (e.g., Peters 2000), as well as its relationship to the homogeneity of mixing, has already been explored in the context of cloud–clear air mixing by Jeffery and Reisner (2006) and Jeffery (2007). They proposed a mathematically strict but computationally intensive model of subgrid-scale mixing suitable for LES simulations. Their results appear broadly consistent with our analysis of the DNS simulations. In the next section, we summarize the numerical model

employed here and describe the simulations. Section 3 presents the analysis procedures and section 4 discusses the results. A brief summary and outlook in section 5 conclude this note.

2. The model, modeling setup, and model simulations

The numerical model, the same as in A04 and A06, is the semi-Lagrangian/Eulerian nonhydrostatic anelastic high-performance model EULAG (Smolarkiewicz and Margolin 1997, 1998; Grabowski and Smolarkiewicz 1996, 2002), which is broadly documented in the literature; see Prusa et al. (2008) for a recent review with comprehensive list of references. For examples of benchmark simulations underlining the veracity of the model, see Wedi and Smolarkiewicz (2006) and Waite and Smolarkiewicz (2008). All simulations reported in this paper apply exclusively the Eulerian (flux form) option of the model because of its desirable conservation properties. The design of numerical simulations augments Herring and Kerr's (1993) numerical study of dry decaying turbulence. The theoretical formulation incorporates a standard incompressible Boussinesq approximation for the dynamics and the detailed microphysics for the thermodynamics. The detailed microphysics applies 16 classes of droplet sizes. Each class is subject to a different sedimentation velocity, and condensation/evaporation takes a finite time depending on the local supersaturation.

The computational domain 0.64^3 m^3 is fixed in all simulations and relatively large grid length (1 cm) is used, as in the majority of simulations presented in A06 (see discussion in section 3 therein). The initial velocity field is constructed from a few low-wavenumber Fourier modes to mimic the large-scale instantaneous input of the TKE; see A04 and A06 for details. The amplitudes selected represent three different large-scale inputs of TKE that correspond to low, moderate, and high intensity levels of the initial TKE. Resulting magnitudes of the initial velocity perturbations are in the range of a few cm s^{-1} for the low TKE input to a few tens of cm s^{-1} for the high TKE input; for illustration see Fig. 1 in section 3 of A04. Initial conditions for the thermodynamic variables prescribe the mixing fraction χ—that is, the ratio of the cloudy and the total volumes, and consequently the initial filament spatial scale—within the low-wavenumber filaments congruent with the velocity field. The basic idea is that these initial conditions represent the input of TKE and scalar variance (including the initial filament scale) from larger scales [e.g., as a result of entrainment in a natural cloud or in laboratory experiments of Malinowski et al. (1998) and Korczyk et al. (2006)]; see the discussion near the end of the introduction to A04 (top of the left column on p. 1278).

To facilitate various mixing conditions, a set of 90 model simulations are performed, some already included in the analysis presented in A06. Table 1 lists all simulations grouped into three sets A, B, and C, with the relative humidity of the dry air held constant in set A and the mixing fraction χ held constant in sets B and C. The TKE level (low, medium, and high) and the initial mean size of cloud droplets are systematically varied in the sets. The changes of the mean droplet size are accomplished by using the same shape of the droplet size distribution (with three consecutive bins containing 25%, 50%, and 25% of the cloud water mixing ratio; see A04 and A06) and by changing the bin width of the droplet spectrum. Such an approach results in the initial mean radius of cloud droplets around 9 μm in the case referred to as regular in Table 1, and radii around 2, 5, and 18 μm in simulations where the bin size was 4 times smaller, 2 times smaller, and 2 times larger than in the regular case, respectively.

3. Analysis

The analysis of all model simulations is conducted in the following way. For each simulation, instantaneous mean (domain-averaged) macrophysical fields (the temperature, water vapor, and velocity) as well as microphysical fields (droplet size distributions) are used to diagnose the turbulent mixing and droplet evaporation time scales. The turbulent mixing time scale is estimated as $\tau_{\rm mix} = (\lambda^2/\epsilon)^{1/3}$ [cf. Eq. (2)], where the length scale λ is taken as the mean scale of cloudy filaments, assumed here to be represented by the mean Taylor microscale for the cloud water (q_c) field. The latter is given by $\lambda = (\lambda_1 + \lambda_2 + \lambda_3)/3$, where $\lambda_i = \langle q_c^2\rangle^{1/2}/\langle(\partial q_c/\partial x_i)^2\rangle^{1/2}$ ($i = 1, 2, 3$ correspond to x, y, and z, respectively; $\langle\cdot\rangle$ denotes the domain average).

The TKE dissipation rate ϵ is estimated in two different ways. First, ϵ is estimated based on the characteristic velocity at the scale λ, $\epsilon = u(\lambda)^3/\lambda$, where—assuming the inertial range scaling—$u(\lambda) = u(L)(\lambda/L)^{1/3}$, with L being the size of the computational domain ($L =$ 0.64 m here) and $u(L)$ being the velocity at the scale L, approximated by the mean TKE; that is, $u(L) = \langle 1/3\,(u^2 + v^2 + w^2)\rangle^{1/2}$. In addition, because for the low TKE, droplet sedimentation out of cloudy filaments may contribute more to the small-scale homogenization than the turbulent stirring, the velocity $u(L)$ is taken as $u(L) = \langle 1/3\,(u^2 + v^2 + w^2)\rangle^{1/2} + v_t(\langle r\rangle)$, where $v_t(\langle r\rangle)$ is the terminal velocity of a droplet with the domain-averaged radius $\langle r\rangle$. An alternative way to estimate the eddy dissipation rate is to use the enstrophy $\Omega = (\nabla \times \mathbf{u})^2$

TABLE 1. The set of model simulations. The first column names various sets; the second gives the input TKE (with L, M, and H denoting low, medium, and high values); the third lists the initial mixing fraction of the cloudy air χ; the fourth gives the initial relative humidity of the clear air; the last column marks the initial spectrum of cloud droplets (with R, L, S, and SS depicting regular, twice larger than regular, and half and quarter of the regular bin size, respectively). See text for details.

Set of simulations	TKE level	Mixing fraction χ	RH of dry air (%)	Droplet size
A1	L	0.13, 0.33 0.43, 0.50, 0.67, 0.87	65	R
A2	M	0.13, 0.33 0.43, 0.50, 0.67, 0.87	65	R
A3	H	0.13, 0.33 0.43, 0.50, 0.67, 0.87	65	R
A4	L	0.13, 0.33 0.43, 0.50, 0.67, 0.87	65	L
A5	M	0.13, 0.33 0.43, 0.50, 0.67, 0.87	65	L
A6	H	0.13, 0.33 0.43, 0.50, 0.67, 0.87	65	L
B1	L	0.50	30, 45, 75, 90	R
B2	M	0.50	30, 45, 75, 90	R
B3	H	0.50	30, 45, 75, 90	R
B4	L	0.50	30, 45, 75, 90	L
B5	M	0.50	30, 45, 75, 90	L
B6	H	0.50	30, 45, 75, 90	L
B7	L	0.50	30, 45, 65, 75, 90	S
B8	M	0.50	30, 45, 65, 75, 90	S
B9	H	0.50	30, 45, 65, 75, 90	S
C1	L	0.50	30, 45, 65, 75, 90	SS
C2	M	0.50	30, 45, 65, 75, 90	SS
C3	H	0.50	30, 45, 65, 75, 90	SS

and to calculate the dissipation rate as $\epsilon = 2\nu\langle\Omega\rangle$, where ν is the molecular viscosity (cf. the appendix in A06). Both ways are employed in the analysis.

The droplet evaporation time scale is defined as in (1) using the domain-averaged radius $\langle r\rangle$ and the relative humidity taken as the average over the cloud-free part of the computational domain. Because the cloud-free part of the domain typically disappears rapidly due to the turbulent stirring and droplet sedimentation, only a fraction of the entire evolution of a single simulation can be used in the analysis. This will be illustrated in the next section.

Centered differencing in time is used to estimate the instantaneous slope of the mixing line on the *r–N* diagram corresponding to the values of $\tau_{\rm mix}$ and $\tau_{\rm evap}$ derived as described above.

4. Results

As an example, Fig. 1 shows results from two contrasting simulations used in the analysis presented in this paper. The figure illustrates the evolution of the domain-averaged TKE, mean volume radius, and mean scale of cloudy filaments λ, as well as the *r–N* diagrams for both simulations. As already discussed in the introduction, the homogeneous mixing corresponds to the horizontal line in the *r–N* diagram (i.e., changing droplet size without changing the number of droplets), whereas the vertical line (reduction of the number without changing the size) implies extremely inhomogeneous mixing. As the *r–N* diagrams show, the mixing between initially separated cloudy and clear air filaments in B3 simulation is close to the homogeneous, whereas extremely inhomogeneous mixing takes place in B7 run. The dots in the figure show time levels used in the analysis; the data from the rest of the simulation are discarded because of the problems with deriving clear-air relative humidity, as mentioned in the previous section.

The main result of the current study is shown in Fig. 2. The figure shows scatterplot of the slope of the mixing line on the *r–N* diagram as a function of the ratio between the turbulent mixing and the droplet evaporation time scales. Each point in the figure represents instantaneous data (such as the mean filament width, mean droplet radius, mean RH of cloud-free air, etc.) taken from all simulations listed in Table 1. The two symbols in Fig. 2 represent results obtained using two distinct ways to estimate the eddy dissipation rate ϵ (i.e., via TKE or enstrophy). It is reassuring to see that both methods used to define the turbulent mixing time scale result in similar relationships, with larger/smaller time scale ratios corresponding to larger/smaller slopes of the mixing line on the *r–N* diagram. This is consistent with the heuristic argument put forward in the introduction. When plotted on a logarithmic scale as in Fig. 2, the spread of points for both the small and large time scale ratios appears substantial. However, one can argue that for practical purposes all slopes smaller than 0.01, or perhaps even 0.1, lead to similar results, that is, large changes in the droplet radius and negligible changes in the number of droplets. In other words, when the slope

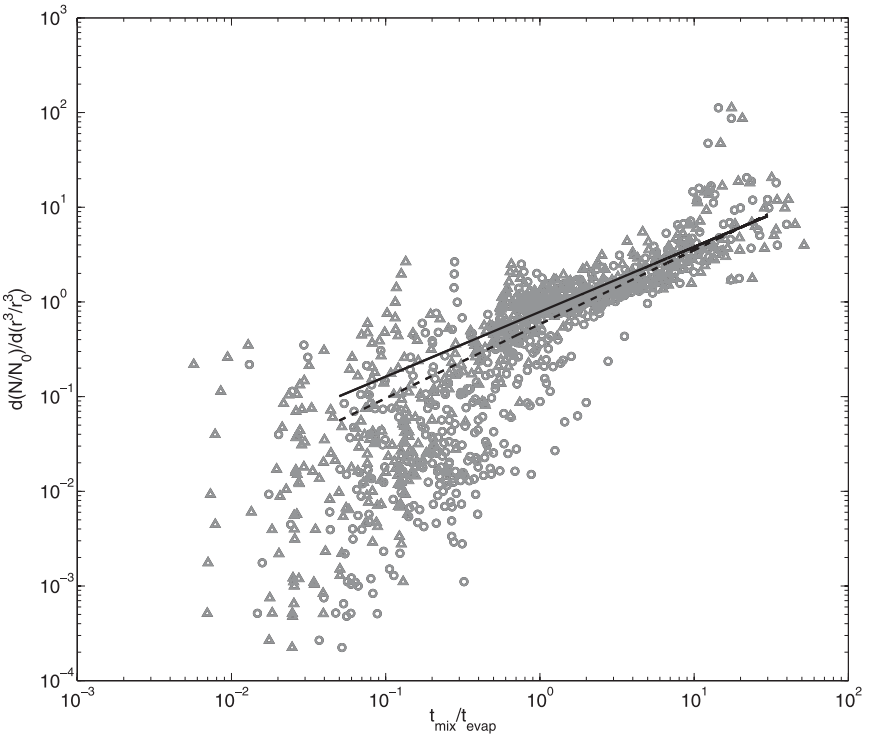

FIG. 2. Scatterplot of the slope of the mixing line on the *r–N* diagram vs the ratio between the turbulent mixing and the droplet evaporation time scales. Each data point represents analysis of instantaneous DNS data as explained in text, with triangles (circles) depicting data points with the mixing time scale calculated using TKE (enstrophy). The solid and dashed lines represent linear fits for either triangles or circles. See text for details.

is smaller than 0.1, the mixing differs insignificantly from the theoretical limit of the homogeneous mixing. Similarly, a slope larger than 100 (and perhaps even 10) implies negligible changes in the mean volume radius of cloud droplets compared to the theoretical limit of the extremely inhomogeneous mixing. An important result is that in the critical range of the slopes—say, between 0.1 and 10—the relationship is relatively tight and thus one can suggest a simple parameterization.

The two lines included in Fig. 2 represent the least squares fits of a straight line for data points bounded by values of 0.05 and 30.0 for the time scale ratios (the horizontal axis) and slopes (the vertical axis). The solid/dashed line is for data points with the eddy dissipation rate ϵ derived using TKE/enstrophy. Their slopes are 0.69 and 0.78, and the intercepts are -0.10 and -0.23, respectively, for solid and dashed lines. However, because of the significant scatter of the data points, as well as the sensitivity of the fitted lines to the bounds selected, the specific relationships implied by the lines plotted in the figure should be treated with caution. For instance, if one takes all data points for the time scale ratios between 0.1 and 10, then the least squares linear fits have slopes of 1.08 and 1.29.

The range of time scale ratios (i.e., Damkoehler numbers) for which the power law seems to hold relatively tightly in Fig. 2 (i.e., a small scatter of data points) is similar to the range for which the model of cloud front evaporation by Jeffery and Reisner (2006) predicts the maximum correlations between subsaturation and droplet concentration at the cloud front (cf. their Figs. 5 and 7). For a Damkoehler number around 5, Jeffery (2007) predicts the mixing regime change from the inhomogeneous to the homogeneous. This qualitatively agrees with the behavior seen in Fig. 2 for $1 < \tau_{\rm mix}/\tau_{\rm evap} < 10$.

5. Summary and outlook

Results obtained in a large series of DNS simulations reveal a robust relationship between the ratio of the turbulent mixing and the droplet evaporation time scales and the slope of the mixing line on the *r–N* diagram. The theoretical limits of the ratio are asymptotic—that is, zero for the homogeneous mixing and infinity for the extremely inhomogeneous mixing. However, the transition from small to large values of the ratio is of key importance. Such a transition happens at every mixing event, from the initial engulfment of the environmental

air, through the turbulent stirring (filamentation), down to the final homogenization through the molecular diffusion and droplet sedimentation.

Arguably, cloud observations should provide insights concerning the homogeneity of mixing in natural clouds. As far as in situ aircraft observations are concerned, the key problem is the speed of the aircraft, which demands ultrafast observing capabilities if one is interested in the cloud microscale. Burnet and Brenguier (2007) discuss results from airborne measurements that illustrate this very aspect. Remote sensing observations, on the other hand, provide information on significantly larger spatial scales (tens to hundreds of meters) and have significant uncertainties [see example of results in McFarlane and Grabowski (2007) and how they compare to in situ observations discussed in Arabas et al. (2009)]. The results of DNS simulations presented here, together with results discussed in Jeffery and Reisner (2006) and Jeffery (2007), provide, to the authors' knowledge, the first attempts to quantify the homogeneity of mixing as a function of the ratio between the turbulent mixing and the droplet evaporation time scales.

The relationship between the time scale ratio and the slope on the *r*–*N* diagram can be used to represent the homogeneity of mixing in LES cloud models. One possibility is to apply the relationship obtained here in a model that combines the approach predicting the scale of cloudy filaments during the turbulent mixing (Grabowski 2007) with the double-moment warm rain microphysics scheme that locally specifies the homogeneity of mixing [see Morrison and Grabowski (2008), particularly Eq. (11) and the accompanying discussion]. Development and applications of such an approach is the subject of ongoing research.

Acknowledgments. This work was partially supported by the Los Alamos National Laboratory's Directed Research and Development Project 20080126DR (MA), the NOAA awards NA05OAR4310107 and NA08OAR-4310543 (WWG), the Polish Ministry of Science and Higher Education (SPM), and the DOE award DE-FG02-08ER64535 (PKS).

REFERENCES

Andrejczuk, M., W. W. Grabowski, S. P. Malinowski, and P. K. Smolarkiewicz, 2004: Numerical simulation of cloud–clear air interfacial mixing. *J. Atmos. Sci.,* **61,** 1726–1739.

——, ——, ——, and ——, 2006: Numerical simulation of cloud–clear air interfacial mixing: Effects on cloud microphysics. *J. Atmos. Sci.,* **63,** 3204–3225.

Arabas, S., H. Pawlowska, and W. W. Grabowski, 2009: Effective radius and droplet spectral width from in-situ aircraft observations in trade-wind cumuli during RICO. *Geophys. Res. Lett.,* **36,** L11803, doi:10.1029/2009GL038257.

Baker, M. B., and J. Latham, 1979: The evolution of droplet spectra and the rate of production of embryonic raindrops in small cumulus clouds. *J. Atmos. Sci.,* **36,** 1612–1615.

——, R. G. Corbin, and J. Latham, 1980: The influence of entrainment on the evolution of cloud droplet spectra: I. A model of inhomogeneous mixing. *Quart. J. Roy. Meteor. Soc.,* **106,** 581–598.

Blyth, A. M., and J. Latham, 1991: A climatological parameterization for cumulus clouds. *J. Atmos. Sci.,* **48,** 2367–2371.

Broadwell, J. E., and R. E. Breidenthal, 1982: A simple model of mixing and chemical reaction in a turbulent shear layer. *J. Fluid Mech.,* **125,** 397–410.

Burnet, F., and J.-L. Brenguier, 2007: Observational study of the entrainment-mixing process in warm convective clouds. *J. Atmos. Sci.,* **64,** 1995–2011.

Chosson, F., J.-L. Brenguier, and L. Schüller, 2007: Entrainment-mixing and radiative transfer simulation in boundary layer clouds. *J. Atmos. Sci.,* **64,** 2670–2682.

Clark, T. L., and W. D. Hall, 1979: A numerical experiment on stochastic condensation theory. *J. Atmos. Sci.,* **36,** 470–483.

Gerber, H., G. Frick, J. B. Jensen, and J. G. Hudson, 2008: Entrainment, mixing, and microphysics in trade-wind cumulus. *J. Meteor. Soc. Japan,* **86,** 87–106.

Grabowski, W. W., 2006: Indirect impact of atmospheric aerosols in idealized simulations of convective–radiative quasi-equilibrium. *J. Climate,* **19,** 4664–4682.

——, 2007: Representation of turbulent mixing and buoyancy reversal in bulk cloud models. *J. Atmos. Sci.,* **64,** 3666–3680.

——, and P. K. Smolarkiewicz, 1996: Two-time-level semi-Lagrangian modeling of precipitating clouds. *Mon. Wea. Rev.,* **124,** 487–497.

——, and ——, 2002: A multiscale anelastic model for meteorological research. *Mon. Wea. Rev.,* **130,** 939–956.

Haman, K. E., S. P. Malinowski, M. J. Kurowski, H. Gerber, and J.-L. Brenguier, 2007: Small scale mixing processes at the top of a marine stratocumulus—A case study. *Quart. J. Roy. Meteor. Soc.,* **133,** 213–226.

Herring, J. R., and R. M. Kerr, 1993: Development of enstrophy and spectra in numerical turbulence. *Phys. Fluids,* **5A,** 2792–2798.

Jeffery, C. A., 2007: Inhomogeneous cloud evaporation, invariance and Damköhler number. *J. Geophys. Res.,* **112,** D24S21, doi:10.1029/2007JD008789.

——, and J. M. Reisner, 2006: A study of cloud mixing and evolution using PDF methods. Part I: Cloud front propagation and evaporation. *J. Atmos. Sci.,* **63,** 2848–2864.

Korczyk, P. M., S. P. Malinowski, and T. A. Kowalewski, 2006: Mixing of cloud and clear air in centimeter scales observed in laboratory by means of particle image velocimetry. *Atmos. Res.,* **82,** 173–182.

Malinowski, S. P., and I. Zawadzki, 1993: On the surface of clouds. *J. Atmos. Sci.,* **50,** 5–13.

——, M. Y. Leclerc, and D. Baumgardner, 1994: Fractal analyses of high-resolution cloud droplet measurements. *J. Atmos. Sci.,* **51,** 397–413.

——, I. Zawadzki, and P. Banat, 1998: Laboratory observations of cloud–clear air mixing at small scales. *J. Atmos. Oceanic Technol.,* **15,** 1060–1065.

——, M. Andrejczuk, W. W. Grabowski, P. Korczyk, T. A. Kowalewski, and P. K. Smolarkiewicz, 2008: Laboratory and modeling studies of cloud–clear air interfacial mixing: anisotropy of small-scale turbulence due to evaporative cooling. *New J. Phys.,* **10,** 075020, doi:10.1088/1367-2630/10/7/075020.

McFarlane, S. A., and W. W. Grabowski, 2007: Optical properties of shallow tropical cumuli derived from ARM ground-based remote sensing. *Geophys. Res. Lett.,* **34,** L06808, doi:10.1029/2006GL028767.

Morrison, H., and W. W. Grabowski, 2008: Modeling supersaturation and subgrid-scale mixing with two-moment bulk warm microphysics. *J. Atmos. Sci.,* **65,** 792–812.

Paluch, I. R., and D. G. Baumgardner, 1989: Entrainment and fine-scale mixing in a continental convective cloud. *J. Atmos. Sci.,* **46,** 261–278.

Peters, N., 2000: *Turbulent Combustion*. Cambridge University Press, 304 pp.

Prusa, J. M., P. K. Smolarkiewicz, and A. A. Wyszogrodzki, 2008: EULAG, a computational model for multiscale flows. *Comput. Fluids,* **37,** 1193–1207.

Siebert, H., K. Lehmann, and M. Wendisch, 2006: Observations of small-scale turbulence and energy dissipation rates in the cloudy boundary layer. *J. Atmos. Sci.,* **63,** 1451–1466.

Slawinska, J., W. W. Grabowski, H. Pawlowska, A. A. Wyszogrodzki 2008: Optical properties of shallow convective clouds diagnosed from a bulk-microphysics large-eddy simulation. *J. Climate,* **21,** 1639–1647.

Smolarkiewicz, P. K., and L. G. Margolin, 1997: On forward-in-time differencing for fluids: An Eulerian/semi-Lagrangian nonhydrostatic model for stratified flows. *Atmos.–Ocean,* **35,** 127–152.

——, and ——, 1998: MPDATA: A finite-difference solver for geophysical flows. *J. Comput. Phys.,* **140,** 459–480.

Squires, P., 1952: The growth of cloud droplets by condensation. *Aust. J. Sci. Res.,* **6,** 66–86.

Waite, M. L., and P. K. Smolarkiewicz, 2008: Instability and breakdown of a vertical vortex pair in a strongly stratified fluid. *J. Fluid Mech.,* **606,** 239–273.

Wedi, N. P., and P. K. Smolarkiewicz, 2006: Direct numerical simulation of the Plumb–McEwan laboratory analog of the QBO. *J. Atmos. Sci.,* **63,** 3226–3252.